Proceedings of
ASME Turbo Expo 2002
June 3-6, 2002, Amsterdam, The Netherlands

GT-2002-30054

OBSERVATIONS OF FLAME BEHAVIOR IN A LABORATORY-SCALE PRE-MIXED NATURAL GAS/AIR GAS TURBINE COMBUSTOR FROM CARS TEMPERATURE MEASUREMENTS

Paul O. Hedman, Daniel V. Flores, and Thomas H. Fletcher
Department of Chemical Engineering, Brigham Young University, Provo, Utah, USA 84602

ABSTRACT

This objective of this study was to obtain instantaneous gas temperature measurements using a coherent anti-Stokes Raman spectrometer (CARS) in a laboratory-scale, gas-turbine combustor (LSGTC) with a pre-mixed, swirl-stabilized, natural gas flame. These measurements complement PLIF measurements of OH radical, and LDA measurements of velocity which are presented in companion papers [1,2]. Gas temperature measurements were obtained at each of four operating conditions (high swirl and medium swirl at fuel equivalence ratios of 0.80 and 0.65). Results of mean and standard deviation measurements are included in this paper for all four test cases. Additionally, example probably density functions (PDF) for the gas temperature at the 40 mm, 60 mm, and 80 mm axial locations are presented for the for the high swirl (HS) $\varphi = 0.80$ case (most stable flame) and the medium swirl (MS) $\varphi = 0.65$ case (least stable flame).

INTRODUCTION

This study was part of a series of laser-diagnostic experiments performed on a common combustion apparatus. Companion studies were performed to measure gas velocities using two-component laser Doppler anemometry (LDA) [3] and to obtain instantaneous planar laser induced fluorescence (PLIF) images of OH [1]. These data were obtained principally for evaluation of comprehensive gas turbine combustion models [4-7]. The work presented here is the result of coherent anti-Stokes Raman spectroscopy (CARS) measurements of gas temperature and selected species concentrations in a laboratory-scale, gas-turbine combustor (LSGTC) with a pre-mixed, swirl-stabilized, natural gas flame at atmospheric pressure. Operating conditions at high swirl and medium swirl at fuel equivalence ratios of 0.80 and 0.65 were studied. This paper reports on the instantaneous, mean, and probability density functions (PDFs) of CARS gas temperature measurements obtained at these four operating conditions.

Past experience at BYU/ACERC has shown that the modeling of combustion behavior is more accurate and proceeds more rapidly when coupled with pertinent, foundational experimental research. The LSGTC simulates many of the key combustor characteristics of commercial gas turbines [8], and provides a realistic flame where model predictions and in situ measurements can be compared. Use of advanced optical diagnostics has permitted multiple, non-intrusive, near-instantaneous CARS measurements of temperature, LDA measurements of velocity, and OH-PLIF images of flame shape. These experimental measurements provide insight into the physical processes that govern the combustion processes, provide direction to the modeling of the combustion process, and have also provided a database suitable for model sub-code evaluation and verification.

The objective of this part of the experimental program was to obtain approximately 1000 instantaneous measurements were obtained at each of about 250 separate *in situ* diagnostic locations in the combustor. The instantaneous measurements were analyzed to obtain mean and standard deviations at each measurement location.

COMBUSTOR TEST FACILITY

The combustion facility used for this study is the same as that used by Hedman and coworkers [1-2, 9-11]. Pyper [12] constructed the laboratory-scale gas turbine test facility, and assisted Warren and Hedman [11] in installing a single Stokes CARS (coherent anti-Stokes Raman Spectrometer) instrument. This CARS instrument was used to make temperature measurements on a practical non-premixed fuel injector from and aircraft jet engine that had been provided by Pratt Whitney Aircraft Company [8] and Wright Patterson Air Force Base [13]. Schmidt and Hedman [14] incorporated a premixed injector and used the burner to make CARS temperature and LDA velocity measurements on a premixed propane/air flame. The facility was further modified for this study to allow investigation of a premixed natural gas/air flame

The LSGTC, illustrated in Figure 1, was designed to reproduce the characteristics found in a modern annular combustor [8]. The combustion chamber consists of a foursided chamber with metal fillets in the corners to more nearly simulate an axisymmetric combustor while maintaining adequate optical access. Each of the four walls can be either a metal plate or a quartz window, depending on the optical access required.

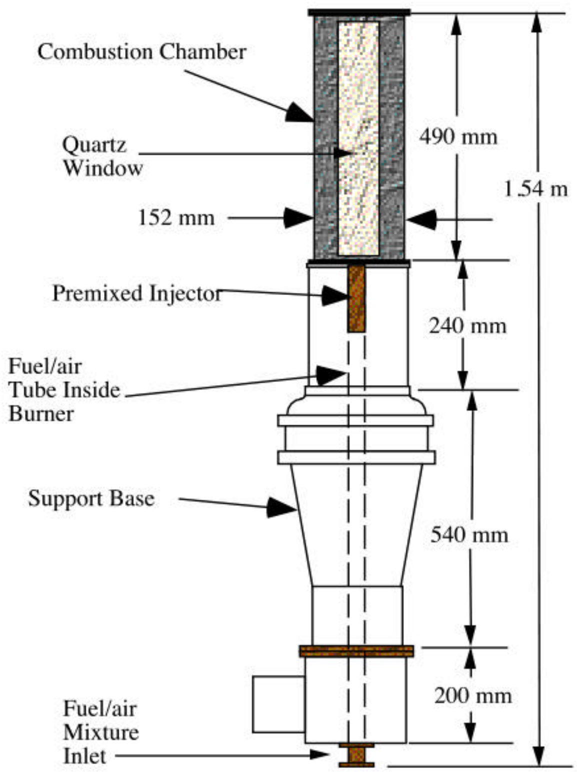

FIGURE 1. SCHEMATIC OF PREMIXED COMBUSTOR (Adapted from Schmidt and Hedman [14])

The premixed swirl injector, illustrated in Figure 2, was located in the center of the combustion chamber base. The injector consisted of a stainless steel tube with a honeycombed brass insert. The brass insert served to smooth the flow as well as provide a flame arrestor in case of flashback in the premixed fuel air mixture. Inserts were installed in the injector to provide different magnitudes of swirl to the inlet flow. The swirler inserts were placed above the brass honeycomb and secured by a threaded post that anchored the swirler to the brass honeycomb. A cap with an 18-mm hole in the center and beveled walls was placed on the top of the steel tube to coalesce the swirling flow at the injector exit. This cap made the burner operate successfully.

Figure 2 also shows a schematic of the two swirl inserts used in this study. The swirl inserts are labeled HS and MS to coincide with the 60 and 45-degree slot angles. The swirl number (SN) is a non-dimensional number that ratios the axial flux of tangential momentum to the axial flux of axial momentum times the equivalent nozzle radius [15]. A swirl number close to zero ($SN << 1$) means the axial momentum is very large compared to the tangential momentum, whereas a very large swirl number ($SN >> 1$) indicates that the axial momentum is small compared to the tangential momentum.

Fuel flow to the burner was measured with a variable area flow meter and is reported in slpm (1 atm, 70 _F). Varying the upstream pressure to a choked flow nozzle controlled the airflow to the burner. The diameter of the choked flow nozzle used for this study was 0.1485 in. and provided airflow rates from 250 to 1000 slpm depending on upstream pressure. Uniform mixing of gaseous fuel and air was assured by: the length of the tube from the mixing point to the burner; by a jet mixer in the feed system; and by the honeycomb flame arrestor. The airflow rate for the four test conditions used in this study was 500 slpm. The stoichiometric ratio was varied by adjusting the flow rate of the natural gas to the injector.

GAS TEMPERATURE MEASUREMENTS

Boyack and Hedman [16] set up a dual Stokes CARS instrument in the BYU Optics Laboratory and used that instrument to measure gas temperature and species concentrations (O_2, CO_2, and CO) in a CO/air diffusion flame. Following Boyack's study, Hedman and Warren [10] set up a single Stokes CARS instrument on the LSGTC and used the instrument to obtain gas temperature measurements in a gaseous propane fueled, non-premixed, practical combustor. Schmidt and Hedman [14] used the single Stokes instrument to make CARS temperature measurements on a premixed propane/air flame. These studies provided the initial starting point for the current CARS system. Haslam and Hedman [17] and Dawson and Hedman [18] modified the single Stokes system (only suited for temperature measurements) to include dual pyromethene dyes in a single Stokes CARS system. The dual dye allowed the Stokes frequencies of CO_2, O_2, CO, and N_2 to be simultaneously excited permitting simultaneous measurement of gas temperature and concentration of CO_2, O_2, and CO to be made. Dawson and Hedman [18] and Flores and Hedman [19] used the modified system to make preliminary temperature and species concentration measurements in a premixed natural gas flame. Flores [20] has made further modifications to the CARS and used the refined system to make the measurements reported in this paper. A subsequent paper that details the concentration measurements is planned.

A simplified figure that illustrates the theoretical aspects of CARS is shown in Figure 5. Coherent anti-Stokes spectroscopy (CARS) is based on Raman scattering of high energy, coherent, laser beams. In general, a pump beam is split into two beams of equal intensity, and crossed with a Stokes beam that is tuned to the particular Raman resonance for the species being probed (e.g. 2331 cm^{-1} for N_2 and 2143 cm^{-1} for CO). Non-linear wave mixing occurs in the diagnostic volume where the three probe beams cross, and a fourth beam is generated at the anti-Stokes frequency for the species being probed. The anti-Stokes spectra contain information that relates to gas temperature and species concentration. The non-linear wave mixing is a vector process, and the laser like anti-Stokes signal leaves the diagnostic volume in a prescribed direction that depends on the vector angles of the pump and Stokes beams. Since the signal is laser like, it can be focused

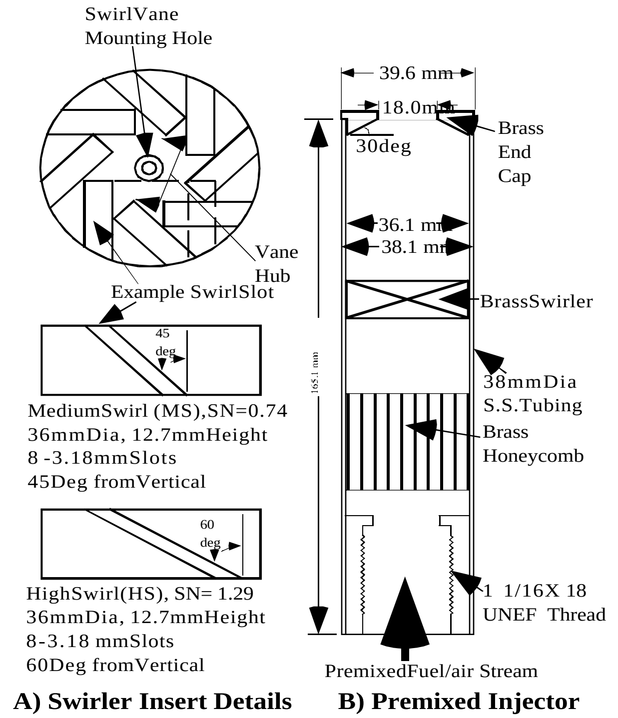

FIGURE 2. SCHEMATIC OF PREMIXED INJECTOR AND MEDIUM AND HIGH SWIRL BLOCK INSERTS (Adapted from Schmidt and Hedman [14])

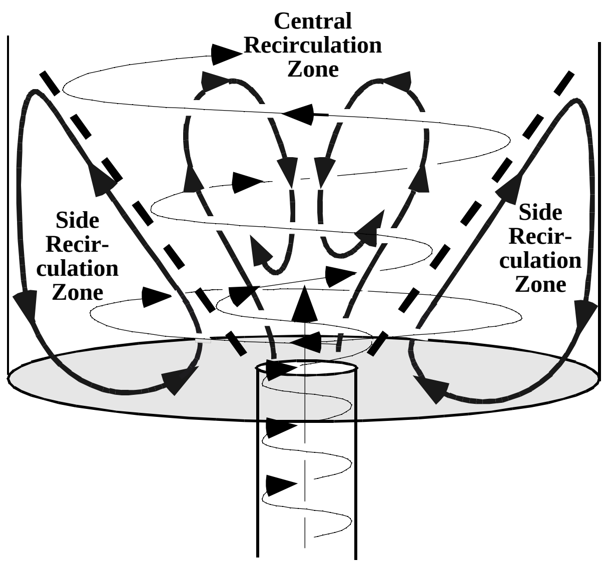

The tornado like nature of the central swirl-stabilized flame is clearly evident. The flame draws gases from downstream forming a central recirculation zone. A side recirculation zone is also formed between the bluff base of the combustor and the side wall.

FIGURE 3. FLOW PATTERNS IN A CONFINED, BLUFF-BASE, PREMIXED, SWIRL-STABILIZED COMBUSTOR (Adapted From Guptka, et al. [15]).

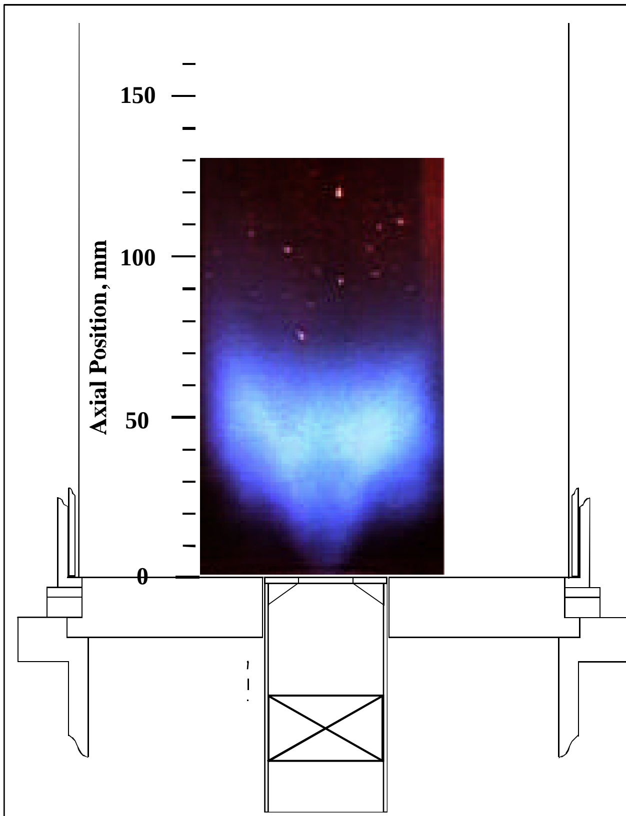

FIGURE 4. EXAMPLE VIDEO IMAGE OF PREMIXED NATURAL GAS/AIR FLAME (MS BURNER, 500 SLPM AIR FLOW RATE, ϕ = 1.0)

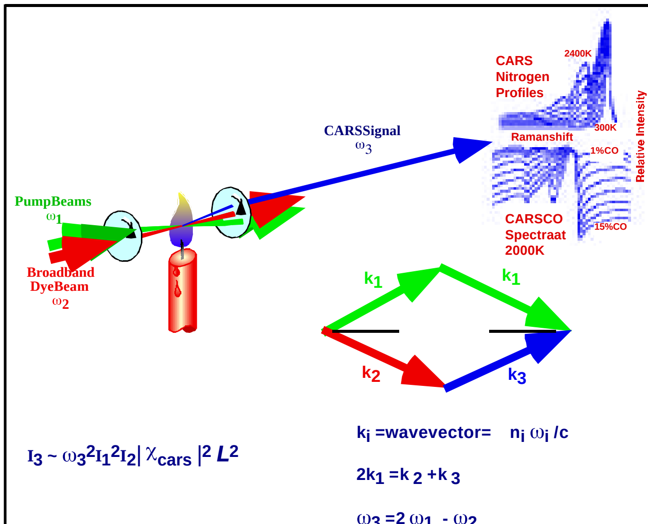

FIGURE5.DETAILSOFCARSSPECTROSCOPY

into a spectrometer for analysis. A detailed discussion of CARS theory and application can be found in Eckbreth [21].

The BYU CARS instrument, shown schematically in Figure 6 as installed on the LSGTC, uses a frequency doubled ND:Yag laser (532 nm) to supply the two pump beams. A portion of the 532 nm laser energy is split off and used to provide the excitation of the Stokes laser. The broad band, dual pyromethene dye laser (pyromethene 597 and 650 from Exciton) is used to simultaneously excite the Raman frequencies of N_2, CO, O_2, and CO_2. The spectrometer used in this study was patterned after the one used by Eckbreth at UTRC [22, 23]. The diagnostic volume had a 200 μm waist and a 1 mm length. The spectra were imaged onto the intensified photodiode array (IPDA) of an EG&G PARC 1421B camera, and recorded to a computer via an EG&G OMA model 1461. The specific characteristics of the IPDA and OMA system were determined by Boyack [23]. Gas temperatures were determined from the N2 CARS spectra using the FTCARS code [24] from SANDIA National Laboratories with modified input and output interfaces. Spectra that were too noisy or that could not be fit well with the FTCARS code were discarded. Flores [20] conducted temperature calibration measurements on air in an electrically heated tube furnace equipped with a Type K thermocouple and a digital readout. Measurements in the range of 300 K to 1000 K resulted in an average error of 30 K and standard deviations of 50 K. Accuracy of the temperature measurements at higher temperatures is thought to be within the usual ± 50 K generally assumed for the CARS technique. The diagnostic volume had a 200 μm waist and a 1 mm length. Additional details of the instrumentation and calibration are given by Flores [19, 20]. This study used the N_2 anti-Stokes spectra to deduce the gas temperatures presented herein. A subsequent paper is planned to present the gas concentrations results determined form the CO, O_2, and CO_2 spectra.

Figure 7 presents the iso-contour mean gas temperature maps for the four cases tested in this study (HS and MS and $\varphi = 0.65$ and 0.80). Figure 7(a) presents the results for the MS $\varphi = 0.65$ (least stable flame) case and Figure 7(d) presents the results for the HS $\varphi = 0.80$ (most stable flame) case. Comparison of these two figures shows the broadest effect of both swirl level, and stoichiometry. The definition of stability used here is in regards to flame extinction rather than the amount of turbulent fluctuations present. The MS $\varphi = 0.65$ (least stable flame) case was quite unstable, and the visible flame would move from a flame attached to the injector inlet to a flame that was lifted up into the combustion chamber. The mean temperature map doesn't show this effect because of the averaging involved. The average temperature contours do show a flame that is higher in the combustion chamber when compared to the HS $\varphi = 0.80$ (most stable flame) case. The peak temperature of the MS $\varphi = 0.65$ (least stable flame) case was also lower (1449 K versus 1648 K) than the HS $\varphi = 0.80$ case.

Comparison of Figures 7(a) and 7(b) or Figures 7(c) and 7(d) show that the increased heat release associated with the higher fuel equivalence ratio (0.80 versus 0.65) had the effect of increasing flame stability causing the vortex core to be closer to the injector inlet. The increased heat release also causes a significant increase in the peak flame temperature.

The effect of swirl on flame structure can be seen by comparing Figures 7(a) and 7(c) or Figures 7(b) and 7(d). The higher swirl level has increased flame stability as evidenced by: 1) the location of the flame vortex (high swirl moves the vortex closer to the injector), and 2) the higher peak flame temperatures associated with the higher swirl level (1550 K versus 1449 K for the $\varphi = 0.65$ cases, and 1648 K versus 1603 K for the $\varphi = 0.80$ cases).

Recirculation zones play a major role in stabilizing a turbulent, premixed natural gas combustor. Hedman and coworkers [1,2] showed that gas moving down into the ignition zone and radially towards the axial centerline improved the stability of the flame. The intensity of the recirculation zones was based on how well the recirculation zones moved hot gases to the middle of the combustion chamber and down into the ignition zone. The vortex structures shown in the gas temperature maps are consistent with the previous observations of OH-PLIF images, and the similar iso-velocity contours shown in the companion studies mentioned above.

The analysis of the approximately 1000 instantaneous gas temperature measurements obtained at each *in situ* measurement location in the flame zone allowed statistical investigation into the turbulent character of the flame to be made. Standard deviations for the gas temperatures were calculated at each location in the combustion chamber and iso-contour plots of standard deviation (σ_T) temperature are shown in Figure 8 for all four test cases. The actual values of σ_T were normalized by the local mean temperature, and the normalized standard deviation results are presented as percent. This treatment is analogous to that done with fluctuating velocity data to determine a local turbulent intensity. Maximum and minimum mean temperatures are also included in Figure 8.

The effects of swirl level, and stoichiometry on gas temperature fluctuations are apparent in these maps. The effect of swirl level on flame structure and stability can be obtained by comparing Figures 8(a) and 8(c) or Figures 8(b) and 8(d). In general, the peak normalized σ_T temperature level is close to the same for all four cases. Within the flame, the highest levels follow the high velocity shear zone that separates the central recirculation zone with the side recirculation zone. This is consistent with the velocity observations made in a companion study [2]. In the velocity study, the highest values of σ_T correlated directly with the high velocity channel that was associated with the vortex flow. Past studies have suggested that a large standard deviation correlated with high turbulence regions [10,14]. In this study, the largest normalized standard deviation temperatures also occurred in the same location as the largest mean velocity measurements [2].

The effect of stoichiometry on flame structure and stability can be obtained by comparing Figures 8(a) and 8(b) or Figures 8(c) and 8(d). In general, the higher heat release associated with the $\varphi = 0.80$ cases resulted in: 1) a reduction of the size of the highly fluctuating zone, and 2) a movement of that zone closer to the injector inlet.

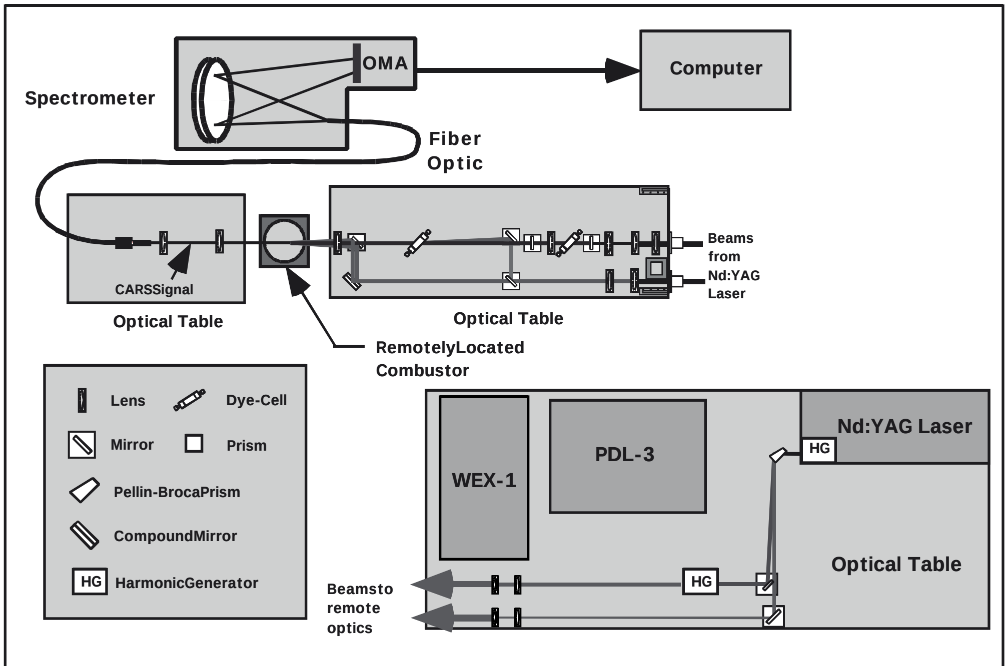

FIGURE 6. SCHEMATIC OF DUAL DYE, SINGLE STOKES CARS INSTALLATION ON THE LABORATORY-SCALE GAS TURBINE COMBUSTOR (LSGTC)

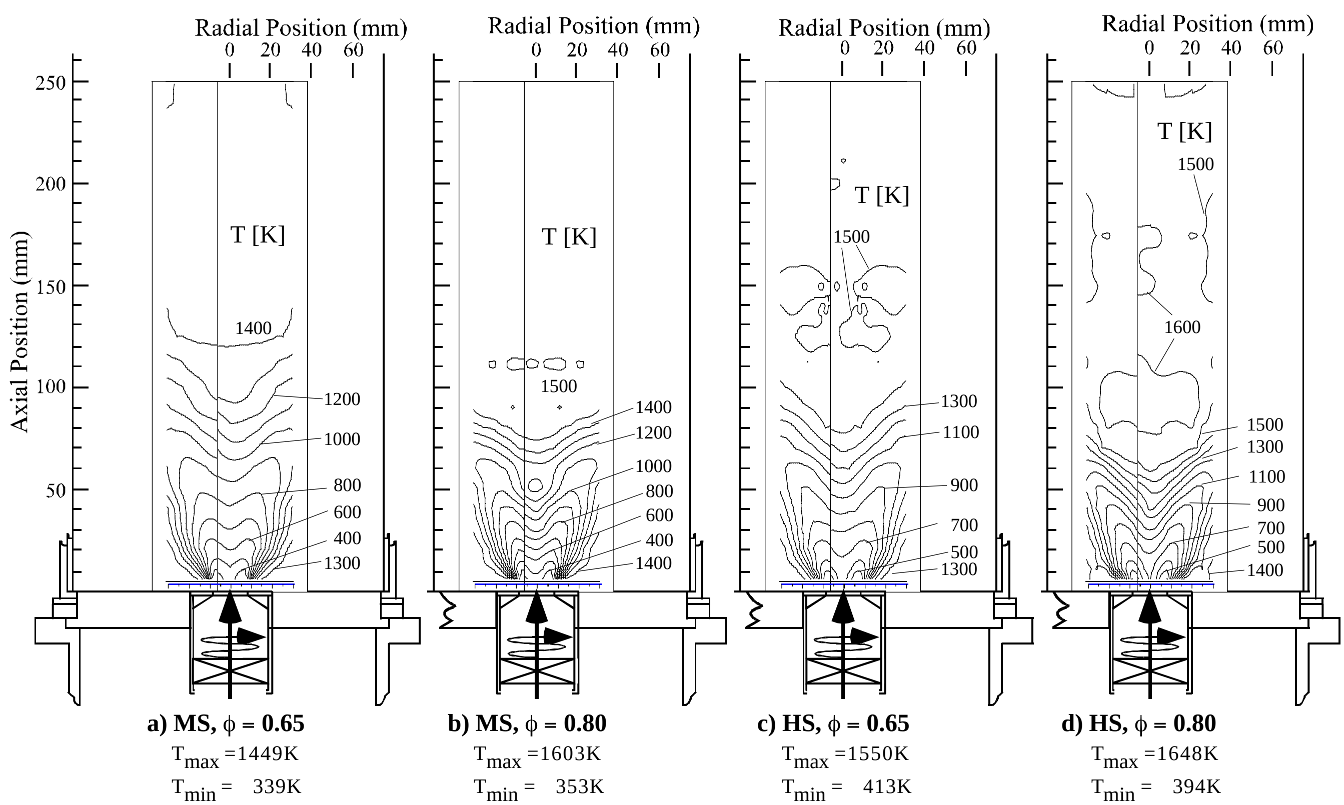

FIGURE 7. CONTOUR MAPS OF MEAN GAS TEMPERATURES FOR THE FOUR TEST CONDITIONS

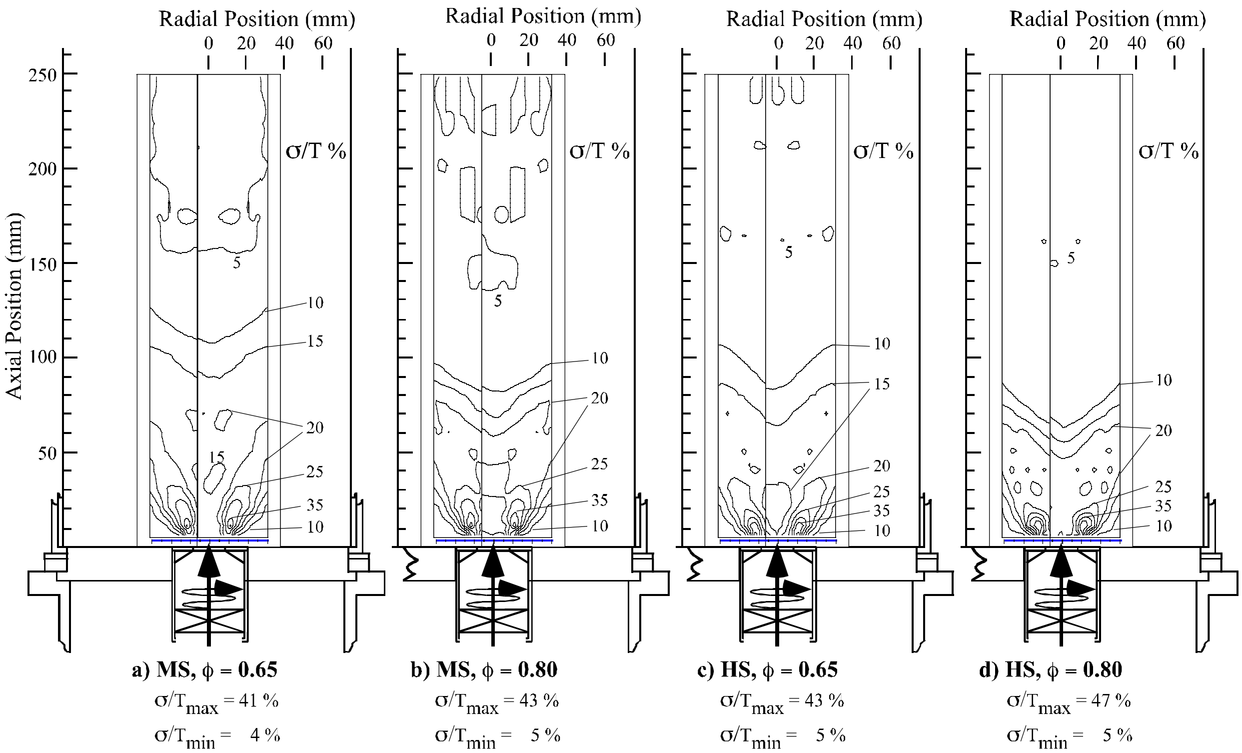

FIGURE 8. CONTOUR MAPS OF NORMALIZED STD DEV GAS TEMPERATURE FOR THE FOUR TEST CONDITIONS

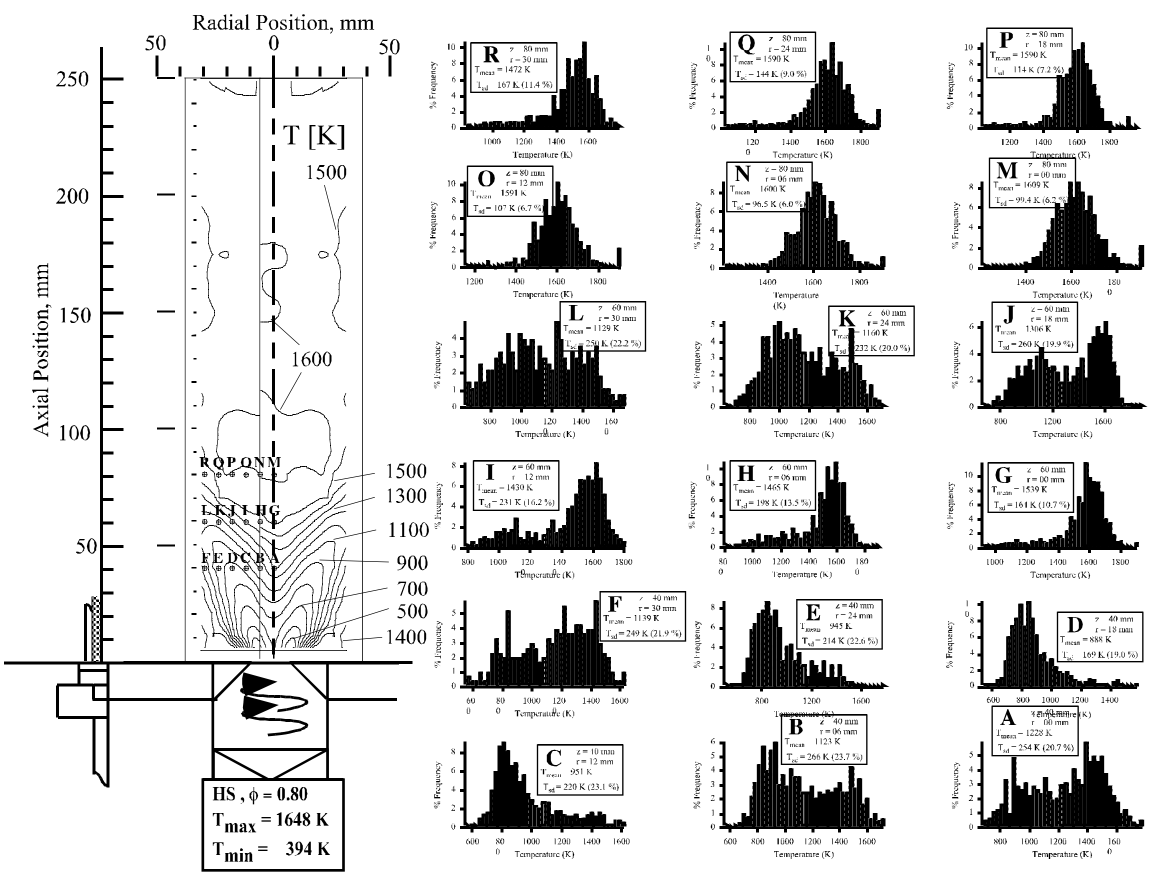

FIGURE 9. MEAN GAS TEMPERATURE CONTOUR MAP AND EXAMPLE TEMPERATURE PDFs, HS, $\phi = 0.80$

Probability distribution functions (PDFs) have been used to describe the characteristics of the fluctuating temperature. Figures 9 and 10 show examples of gas temperature PDFs at axial locations of 40 mm, 60 mm, and of 80 mm and radial positions from the centerline to a 30 mm radial location for the MS φ = 0.65 and HS φ = 0.80 cases. Additional PDF results are included in the dissertation by Flores [20]. Labeled on the PDF are: the axial position, radial position, mean gas temperature (K), standard deviation temperature (K), and normalized standard deviation temperature (%).

In Figure 9, the PDFs generally do not exhibit a Gaussian distribution. The distribution in a single identifiable zone (central recirculation zone or side recirculation zone) seems to follow a beta distribution. As with the velocity distributions [2], the distributions that bridged the two recirculation zones tended to have a bimodal PDF. Comparison of Figure 9 distributions E and F (40 mm) show that these two PDF distributions are clearly on opposite sides of the boundary between the central and side recirculation zones. At a higher position (80 mm), distributions M, N, and O all show a wide distribution that has a bimodal character. This suggests that in the higher part of the flame, there was a significant side to side fluctuation, even though the normalized standard deviation was not large, that shifted the side and central recirculation zones back and forth across the diagnostic locations.

Figure 10 presents similar PDF results for the HS φ = 0.80 case. Since the vortex is more coalesced near the injector for the HS φ = 0.80 case, the bimodal character is easier to identify. Attention is drawn to locations A and B (40 mm) where there is a bimodal character to the PDF distribution even though these locations are near the centerline. Locations C, D, and E (also at 40 mm) reflect distributions in the high velocity region where cooler un-reacted gases are being brought into the combustion chamber. Location F shows a bimodal character, but seems to be dominated by a higher temperature region associated with the side recirculation zone. The distributions at locations G, H, and I (60 mm) are dominated by a high temperature zone associated with the central recirculation zone. However, at locations J, K, and L (also at 60 mm), the distributions have the bimodal character associated with components form both the central and side recirculation zones. Higher in the burner (80 mm) the distributions are nearly Gaussian in shape, and of nearly the same magnitude. This suggests that for this test condition, the combustion was nearly complete and near uniform flow had been achieved. In Figure 9 at this 80 mm location, the mean temperatures showed greater variation with radius, and were much below the final peak temperature in the burner. The PDF observations support the conclusion of strong shear layers in the combustion chamber with bimodal distributions across the shear layer between the central and side recirculation zones.

CONCLUSIONS

The general objective of this study was to gain insight into the flow structure of a turbulent, swirling, premixed natural gas/air combustor by obtaining specific *in situ* temperature data. A combustion chamber that reproduces the characteristics found in a modern annular gas turbine combustor was used to investigate the characteristics of a premixed natural gas/air flame using CARS at four operating conditions (HS and MS at φ = 0.65 and 0.80). A dual dye, single Stokes CARS system was developed and successfully used to collect spectral data on N_2, CO, O_2 and CO_2. The N_2 data were used to make about 1000 instantaneous gas temperature measurements at each of about 250 *in situ* locations in the premixed natural gas burner for each of the four test conditions.

Photographic, video recordings, and PLIF images of OH and velocity maps all showed a wide variation in flame shape for different combinations of swirl number and fuel equivalence ratio. The variations in flame shapes are primarily a result of the effect of the swirl intensity and fuel equivalence ratio on the flow field, with the magnitude of the airflow rate being of secondary importance. The CARS gas temperature measurements confirmed these observations. Operation at φ = 0.80 produced the most stable flames (with respect to flame extinction) with both HS and MS injectors. The flame with the HS injector was more coalesced and closer to the injector than with the MS injector. At φ = 0.65, the flame was quite unstable for both swirl injectors. With the MS injector, the flame would oscillate between two different flame structures, one that was more or less attached to the vortex funnel, and one that was lifted well above the vortex funnel. The MS case at φ = 0.65 was at the very edge of the lean flammability limit, and would on occasion extinguish. The mean temperature contours for the MS φ = 0.65 show a flame that is higher in the combustion chamber when compared to the HS φ = 0.80 (most stable flame) case. The peak temperature of the MS φ = 0.65 (least stable flame) case was also lower (1449 K versus 1648 K). The higher swirl level has increased flame stability and moved the location of the flame vortex (high swirl closer to injector) and caused higher peak flame temperatures with the higher swirl level (1550 K versus 1449 K for the φ = 0.65 cases, and 1648 K versus 1603 K for the φ = 0.80 cases). Recirculation zones play a major role in stabilizing a turbulent, premixed natural gas combustor. The vortex structures shown in the gas temperature maps are consistent with the previous observations of OH-PLIF images, and the similar iso-velocity contours shown in the companion studies.

The highest levels of normalized standard deviations in temperature follow the high velocity shear zone that separates the central recirculation zone with the side recirculation zone. This is consistent with the velocity observations made in a companion study [2]. The higher heat release associated with the φ = 0.80 cases resulted in a reduction of the size of the highly fluctuating zone, and a movement of that zone closer to the injector inlet.

Probability distribution functions (PDFs) have been used to describe the characteristics of the fluctuating temperature. The PDFs generally don't have a Gaussian distribution for the MS φ = 0.65 case. The distribution in a single identifiable zone (central recirculation zone or side recirculation zone) has a beta distribution. The distributions that bridged the two recirculation zones had bimodal PDFs.

The vortex is more coalesced near the injector for the HS φ = 0.80 case, and the bimodal distribution more pronounced. Higher in the burner (80 mm) the distributions are nearly

Gaussian in shape, and of nearly the same magnitude. This suggests that the combustion was nearly complete for this test condition and that near uniform flow had been achieved. This was not true for the 80 mm MS $\varphi = 0.65$ case where the mean temperatures showed greater variation with radius, and were much below the final peak temperature in the burner. The PDFs observations support the conclusion of strong shear layers in the combustion chamber with bimodal distributions across the shear layer between the central and side recirculation zones.

ACKNOWLEDGMENTS

This paper presents results from a study that was funded in part by a U.S. Department of Energy's (DOE) Advanced Turbine Systems (ATS) program and with additional support by the Brigham Young University (BYU) Advanced Combustion Engineering Research Center (ACERC). This study was part of a more comprehensive effort by the U.S. Department of Energy's (DOE) Advanced Turbine Systems (ATS) program to develop advanced high efficiency gas turbines that demonstrated low pollution emissions.

REFERENCES

1. Hedman, P. O., Fletcher, T. H., Graham, S. G., Timothy, G. W., Flores, D. V., and Haslam, J. K., 2002 "Observations of Flame Behavior in a Laboratory-Scale Pre-mixed Natural Gas/Air Gas Turbine Combustor from PLIF Measurements of OH," Paper GT-2002-20052, ASME International Gas Turbine and Aeroengine Congress and Exposition, Amsterdam, The Netherlands.
2. Hedman, P. O., Murray, R. L., and Fletcher, T. H., 2002, "Observations of Flame Behavior in a Laboratory-Scale Pre-mixed Natural Gas/Air Gas Turbine Combustor from LDA Velocity Measurements," Paper GT-2002-20053, ASME International Gas Turbine and Aeroengine Congress and Exposition, Amsterdam, The Netherlands.
3. Murray, R. L., 1998, “Laser Doppler Anemometry Measurements in a Turbulent, Premixed, Natural Gas/Air Combustor,” M. S. Thesis, Chemical Engineering Department, Brigham Young University, Provo, Utah.
4. Cannon, S. M., Brewster, B. S., and Smoot, L. D., 1998, “Stochastic Modeling of CO and NO in Premixed Methane Combustion,” Combustion and Flame, Vol. 113, pp. 135-146.
5. Cannon, S. M., Brewster, B. S., and Smoot, L. D., 1999, “PDF Modeling of Lean Premixed Combustion Using In Situ Tabulated Chemistry,” Combustion and Flame, Vol. 119, pp. 233-252.
6. Mallampalli, H. P., Fletcher, T. H., and Chen, J. Y., 1998, Evaluation of CH_4/NO_x Reduced Mechanisms Used for Modeling Lean Premixed turbulent Combustion of Natural Gas,” ASME Journal of Engineering for Gas Turbines and Power, Vol. 120, pp. 703-712.
7. Meng, F. L., Brewster, B. S., and Smoot, L. D., 1997, “Comprehensive Model for Lean Premixed Combustion in Industrial Gas Turbines – Part II. Application,” Spring 1997 Meeting of the Western States Section/The Combustion Institute, Sandia National Laboratories, Livermore, California.
8. Sturgess, G. J., Sloan, D. G., Lesmerises, A. L., Heneghan, S. P., and Ballal, D. R., 1992, “Design and Development of a Research Combustor for Lean Blowout Studies,” ASME Journal of Engineering for Gas Turbines and Power, Vol. 114, pp. 13-19.
9. Hedman, P. O., Sturgess, G. J., Warren, D. L., Goss, L. P., and Shouse, D. T., 1995, “Observations of Flame Behavior from a Practical Fuel Injector Using Gaseous fuel in a Technology Combustor,” ASME Journal of Engineering for Gas Turbines and Power, Vol. 117, pp. 441-452.
10. Hedman, P. O., and Warren, D. L., 1995, “Turbulent Velocity and Temperature Measurements from a Gas-Fueled Technology Combustor with a Practical Fuel Injector,” Combustion and Flame, Vol. 100, pp. 185-192.
11. Warren, D.L., and Hedman, P. O., 1997, “Differential Mass and Energy Balances in the Flame Zone from a Practical Fuel Injector in a Technology Combustor,” ASME Journal of Engineering for Gas Turbines and Power, Vol. 119, pp. 352-361.
12. Pyper, D. K., 1994, "The Study of Non-Swirl and Swirl Non-Premixed Flame Stability Near Lean Blow Out and the Design of a Research Combustion Facility," M. S. Thesis, Mechanical Engineering Department, Brigham Young University, Provo, Utah.
13. Roquemore, W. M., 1992. Personal Communication, Wright Laboratory, Wright Patterson Air Force Base, Dayton, Ohio.
14. Schmidt, S. E., and Hedman, P. O., 1995,"CARS Temperature and LDA Velocity Measurements in a Turbulent, Swirling, Premixed Propane/Air Fueled Model Gas Turbine Combustor," Paper Number 95-GT-64, ASME International Gas Turbine and Aeroengine Congress and Exposition, Houston, Texas.
15. Gupta, A. K., Lilley, D. G., and Syred, N., 1994, Swirl Flows, Abacus Press, Kent, United Kingdom.
16. Boyack, K. W., and Hedman, P. O., 1990, "Dual-Stokes CARS System for Simultaneous Measurement of Temperature and Multiple Species in Turbulent Flames," Twenty-Third Symposium (International) on Combustion, The Combustion Institute, Pittsburgh, PA..
17. Dawson, R. W., and Hedman, P. O., 1996, “A Technique for Determining Instantaneous N_2, CO, O_2, CO_2, and H_2O Species Concentrations Using Multiplex CARS in Premixed Gaseous Flames,” Paper WSS/CI 96F-087, Fall Meeting of the Western States Section of the Combustion Institute, The University of Southern California, Los Angeles, California (October 28-29).
18. Haslam, J. K., and Hedman, P. O., 1996, “The Use of Two Pyromethene Dyes in a Single Stokes Dye Laser to Make CARS Temperature and Multiple Species (CO, CO_2, O_2, and N_2) Concentration Measurements,” Paper WSS/CI 96F-086, Fall Meeting of the Western States Section of the Combustion Institute, The University of Southern California, Los Angeles, California (October 28-29).

19. Flores, D. V., and Hedman, P. O., 1996, "Simultaneous Measurements of Temperature and Species Concentrations on Premixed natural Gas Flames Using a Dual Dye, Single-Stokes CARS System," Paper WSS/CI 96F-088, Fall Meeting of the Western States Section of the Combustion Institute, The University of Southern California, Los Angeles, California (October 28-29).
20. Flores, D. V., 2002, Ph.D. Dissertation, In Progress, Chemical Engineering Department, Brigham Young University, Provo, Utah 84602.
21. Eckbreth, A. C., 1996, Laser Diagnostics for Combustion Temperature and Species, 2nd Edition, Gordon and Breach Publishers, Amsterdam, The Netherlands.
22. Eckbreth, A. C., 1985, personal communication.
23. Boyack, K. W., 1990, "A Study of Turbulent Nonpremixed Jet Flames of CO/N_2 Using Coherent Anti-Stokes Raman Spectroscopy," Ph.D. Dissertation, Chemical Engineering Department, Brigham Young University, Provo, Utah 84602.
24. Palmer, R. E., 1989, "The CARSFT Computer Code for Calculating Coherent Anti-Stokes Raman Spectra: User and Programmer Information," Sandia Report SAND89-8206, Sandia National Laboratories, Livermore, California.

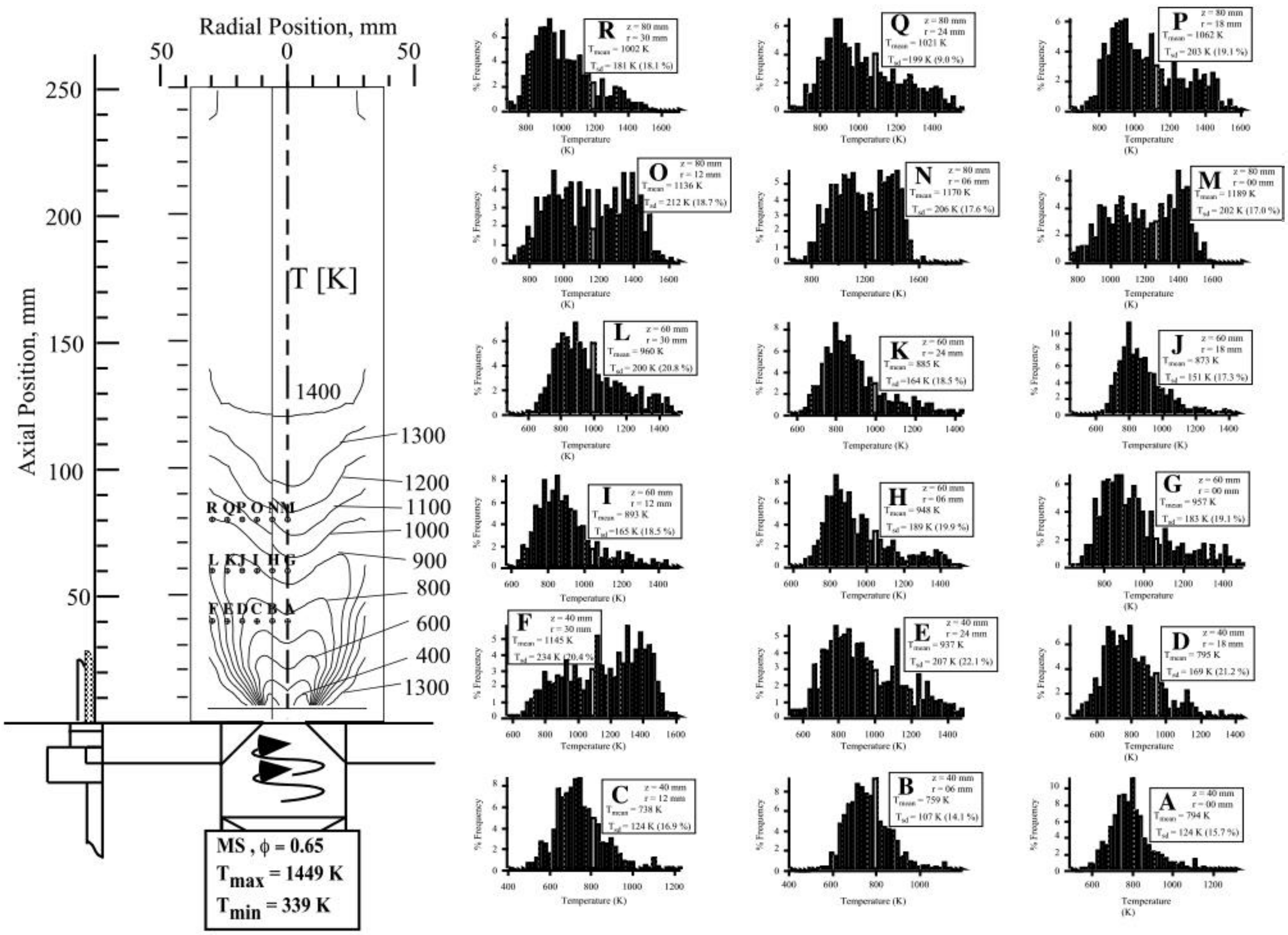

FIGURE 10. MEAN GAS TEMPERATURE CONTOUR MAP AND EXAMPLE TEMPERATURE PDFs, MS, $\phi = 0.65$